Ray and wave chaos in asymmetric resonant optical cavities

Jens U. Nöckel & A. Douglas Stone

Department of Applied Physics, Yale University, New Haven, Connecticut 06520-8284, USA

Optical resonators are essential components of lasers and other wavelength-sensitive optical devices. A resonator is characterized by a set of modes, each with a resonant frequency ω and resonance width $\delta\omega = 1/\tau$, where τ is the lifetime of a photon in the mode. In a cylindrical or spherical dielectric resonator, extremely long-lived resonances [1] are due to 'whispering gallery' modes in which light circulates around the perimeter trapped by total internal reflection. These resonators emit light isotropically. Recently, a new category of asymmetric resonant cavities (ARCs) has been proposed in which substantial shape deformation leads to partially chaotic ray dynamics. This has been predicted [2–4] to give rise to a universal, frequency-independent broadening of the whispering-gallery resonances, and highly anisotropic emission. Here we present solutions of the wave equation for ARCs which confirm many aspects of the earlier ray-optics model, but also reveal interesting frequency-dependent effects characteristic of quantum chaos. For small deformations the lifetime is controlled by evanescent leakage, the optical analogue of quantum tunneling [5]. We find that the lifetime is much shortened by a process known as 'chaos-assisted tunneling' [6,7]. In contrast, for large deformations ($\sim 10\%$) some resonances are found to have longer lifetimes than predicted by the ray chaos model due to "dynamical localization" [8].

The prediction of universal behavior of the whispering gallery resonances is derived from the limit of ray optics in which the wavelength of the light, λ, is much shorter than the radius of curvature of the ARC. Here for simplicity we will focus on the effectively two-dimensional case of a deformed cylindrical resonator as in Fig. 1 (top); the case of deformed spheres (e.g. liquid droplets) in the ray limit has been discussed elsewhere [3]. When the cylinder is undeformed (circular), the angle of incidence χ is conserved at each collision and escape occurs isotropically by the exponentially slow process of evanescent leakage. When the cylinder is sufficiently deformed a new decay process, refractive escape, becomes possible [2,4] in which a ray initially in a whispering gallery trajectory diffuses chaotically in phase space until it reaches the critical angle, $\chi_c = \sin^{-1}(1/n)$, (where n is the refractive index of the dielectric) and is refracted out of the resonator. This is illustrated schematically in Fig. 1 (bottom). Since no refractive escape is allowed for $\chi > \chi_c$, the ray dynamics is equivalent to the non-linear dynamics of a point mass undergoing specular reflection from the walls of a two-dimensional "billiard" [9]. For smooth convex deformations from a circle this dynamics becomes increasingly chaotic with increasing deformation according to the KAM (Kolmogorov-Arnold-Moser) scenario [4,10,11]. One stage in this evolution is shown in the Poincaré sur-

face of section (Fig. 2a). Initially, small regions of chaotic behavior appear near unstable periodic orbits which al-
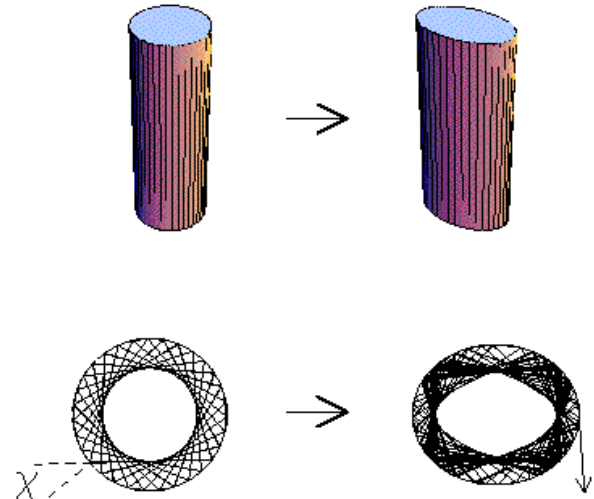

FIG. 1 Top, deformation of a dielectric cylinder of radius R to make an asymmetric resonant cavity (ARC). All results below are for a quadrupolar deformation of the cross-section, so that the radius as a function of angle $r(\phi) = r_0(1 + \epsilon \cos 2\phi)$ (where $\epsilon < 0.2$ measures the size of the deformation and $r_0(\epsilon)$ is chosen to maintain a fixed area). Bottom, regular and chaotic ray trajectories in the plane perpendicular to the cylinder axis for a whispering gallery orbit for $\epsilon = 0, \epsilon = 0.1$; the chaotic trajectory eventually escapes refractively when the sine of the angle of incidence, $\sin \chi < 1/n$.
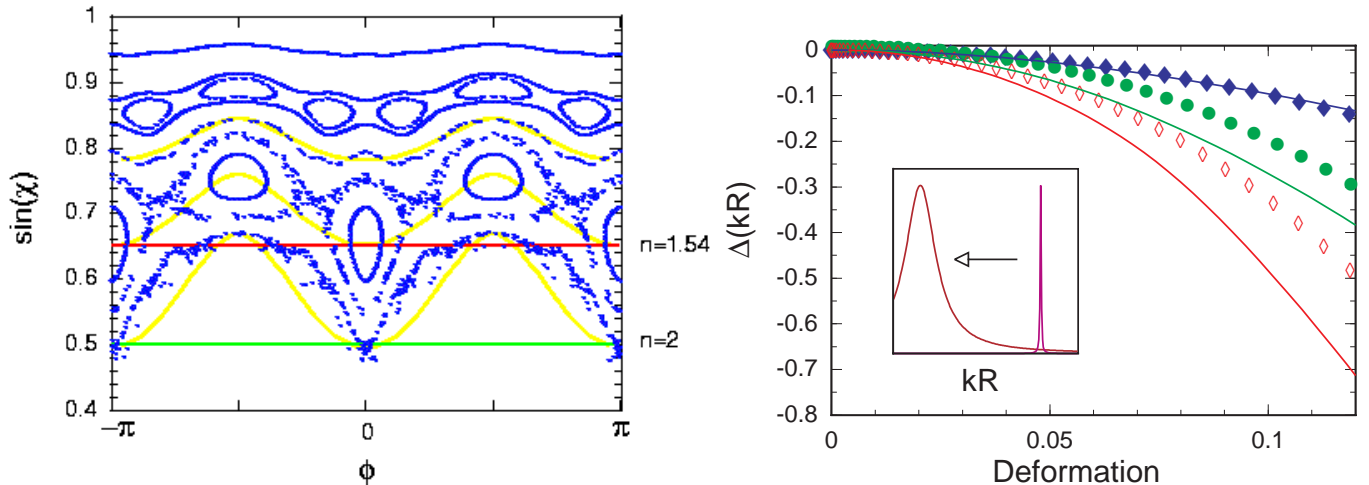
FIG. 2 *a*, Partial Poincaré surface of section showing phase space ray dynamics for several trajectories for $\epsilon = 0.072$. The $\sin\chi$ and the angular position ϕ are recorded at each collision. The green and red horizontal lines represent the critical lines $\sin\chi = 1/n$ for refractive escape for $n = 2, 1.54$. "Islands" indicate trajectories oscillating around stable periodic orbits. Unbroken KAM curves appear above $\sin\chi \approx 0.8$; no whispering gallery orbit can cross such a curve. Trajectories below $\sin\chi \approx 0.8$ lying outside of islands are all chaotic, but when they are followed for 100-200 reflections (as above) they remain near the the adiabatic KAM curves predicted by Eq. (1) (yellow); except when islands intersect the relevant curve (see the discusssion of peak-splitting in Fig. 4 legend). *b*, Shift in resonance frequency with deformation from exact numerical solution of the wave equation for the ARC resonances (solid lines) and from eikonal approximation for the bound states (symbols, adjusted to agree at $\epsilon = 0$). Units of frequency are $kR = 2\pi R/\lambda$ where λ is the wavelength outside the dielectric. For $\epsilon = 0$, the resonances are at $kR \approx 12.1, 27.5, 44.6$ (blue,green, red). Inset schematic shows the generic redshift and broadening of these resonances with deformations. The redshift is easily understood: the approximate condition for a whispering gallery resonance is that an integer number of wavelengths fit around the perimeter (see Fig. 4a). As the ARC is deformed for fixed area the perimeter increases requiring the wavelength to increase.

ternate with stable orbits and their associated islands, but any chaotic trajectory is confined to a small separatrix region near the islands by KAM curves (which correspond to families of regular quasi-periodic orbits). As the deformation increases these KAM curves break up, allowing refractive escape of whispering gallery orbits. Because ray optics describes the limit $\lambda \to 0$, the escape rate due to this process is independent of λ and should be the same for all resonances corresponding to the same set of whispering gallery orbits.

To compare the previous model derived from ray optics [2,4] to solutions of the wave equation we have to overcome a fundamental problem. In regular (integrable) systems a set of trajectories on a KAM curve corresponds to a set of quantized solutions of the wave equation; these solutions are obtained by finding the KAM curves for which the conserved actions are appropriately quantized [12]. For general chaotic systems there exists no such correspondence [12]. For ARC resonances we propose here a method for establishing an approximate correspondence. It is known for 2D convex billiards that the regular orbits which follow KAM curves and generate caustics in the real-space ray motion are well-described by an adiabatic approximation [13]. The (adiabatic) KAM curves representing whispering gallery trajectories in the surface of section of Fig. 2*a* are given by:

$$\sin\chi(\phi) = \sqrt{1 - (1 - S^2)\,\kappa(\phi)^{2/3}}. \tag{1}$$

where $0 < S < 1$ parameterizes the adiabatic curve and $\kappa(\phi)$ is the curvature of the ARC boundary at an azimuthal angle ϕ. Although for the deformations of interest the relevant adiabatic curves are "broken" and the long-time behavior of a chaotic whispering gallery orbit departs strongly from Eq. (1), we find that for intermediate times ($\sim 100 - 500$ collisions) the orbit still follows closely the nearest adiabatic curve.

Thus we propose that the frequency of the resonance will be well-described by the standard semiclassical (eikonal) quantization of the integrable dynamics defined by the adiabatic approximation, even though the resonance lifetime is crucially dependent on the slow chaotic diffusion away from this curve. With this assumption, the resonance frequency can be calculated as a function of deformation by a variant of the eikonal technique of ref. 14; good agreement with exact numerical solutions is found (Fig. 2*b*). The mode indices (quantized actions) are fixed to their values at zero deformation and the calculation yields both the resonance frequency and the adiabatic curve (value of S) corresponding to a given resonance. This adiabatic curve then defines the initial conditions for our ray calculations of the lifetime of a given resonance.

Using the ray model for the resonance lifetime, we

2

calculate the mean escape time of an ensemble of rays launched with uniform density on the appropriate adiabatic curve. At each collision a ray is allowed to escape with a transmission probability (see Fig. 3 legend) which takes into account both the direct tunneling which is present without deformation, and the Fresnel scattering once $\sin\chi < 1/n$. In Fig. 3 the ray prediction for the lifetime is compared to exact wave solutions for three resonances associated with the same initial adiabatic curves but very different wavelengths. Note that above the critical deformation for refractive escape the widths of all the resonances agree up to factors of order unity and also agree well with the ray model. This confirms the universality of the broadening arising from chaotic diffusion.
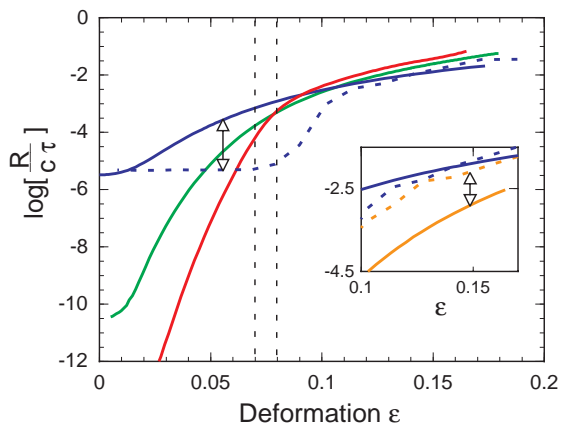

FIG. 3 Logarithm of inverse resonance lifetimes (in units of R/c) vs. deformation for the same resonances as in Fig. 2b (same color coding), determined numerically. All three resonances correspond to an initial adiabatic curve with $\sin\chi_0 \approx 0.8$. Dashed blue line is the result for this adiabatic curve from the ray-optics model for the $kR = 12.1$ resonance. The escape probability for collisions at $\sin\chi$ is determined by the semiclassical relation $\sin\chi = m/nkR$ and the known resonance lifetimes of the cylinder for angular momentum m (J.U. Nöckel et al., in preparation). Dashed black lines delimit the cross-over region from evanescent to refractive escape when the last intervening KAM curve breaks; as expected all three resonances have approximately the same lifetime above this deformation. The discrepancy at small ϵ (see arrow) is indicative of chaos-assisted tunneling. *Inset*: Expanded scale showing the resonance with $kR \approx 12.1$ and its agreement with the ray-optics approximation (dashed blue) at high deformations. Also shown (brown) is a resonance with $\sin\chi_0 \approx 0.9$, $kR \approx 33.2$, which has a substantially longer lifetime than predicted by the ray-optics model (dashed brown). The difference marked by the arrow indicates the dynamical localization of photons.

However, Fig. 3 indicates two significant effects which *do* depend on wavelength and are beyond the ray model. First, we note that for small deformations, where only tunneling escape is possible, the exact resonance width actually increases much faster than predicted by the ray model. We believe that this is due to chaos-assisted tunneling [6,7], since the direct (angular-momentum-conserving) tunneling is taken into account by the ray model. All evanescent (tunneling) processes are forbidden within ray optics, however the probability of such a process decreases exponentially with the tunneling distance. Consider the whispering gallery orbit traversing the surface of section of Fig. 2a at $\sin\chi \approx 0.9$. This orbit lies on an unbroken adiabatic curve and hence will never escape according to ray optics. However a wavepacket following this orbit has a chance to tunnel through this dynamical barrier to the edge of the chaotic region at $\sin\chi = 0.8$. From this region, chaotic diffusion will take the wave-packet without any further tunneling down to the critical angle for refractive escape. Due to the shortness of the tunneling step, this new escape path, which is introduced by the presence of chaos in a classically inaccessible region of phase space, strongly enhances the evanescent leakage of these resonances.

Second, we find that for resonances with the longest lifetimes the ray model predicts too short a lifetime at large deformations. At large deformations refractive ray escape is allowed, so the longer lifetime of the wave solution indicates that this classically-allowed escape is being suppressed. Precisely such an effect, known as dynamical localization, has been studied extensively in the theory of quantum chaos. Unlike a particle (or ray), a wave is able to explore simultaneously multiple paths while undergoing chaotic diffusion. Typically after a characteristic time these multiple paths destructively interfere suppressing further diffusion. Such an effect has been observed indirectly through the suppression of electron ionization in atomic hydrogen in an intense microwave electric field [8].

Finally, we briefly analyse the onset of directional emission shown in Fig. 4, and discussed in more detail elsewhere [15]. As shown in Fig. 2a, the dynamics of whispering gallery orbits consists of a rapid motion along adiabatic curves and a slow chaotic diffusion transverse to them. Hence the whispering gallery orbits of interest, which begin far from the critical line $\sin\chi = 1/n$, will diffuse slowly until the adiabatic curve is reached which is tangent to the critical line and then will escape rapidly near the points of tangency (Fig. 2a). These points correspond to the points of maximum curvature of the ARC according to Eq. (1). Rays escaping near the critical angle are emitted roughly tangent to the surface predicting strong emission maxima in the far-field in directions tangent to the points of maximum curvature (Fig. 4a). This model predicts that all ARC whispering gallery resonances will have approximately the same directional emission pattern for a given index of refraction (Fig. 4b). This universality persists even when the adiabatic approximation breaks down, as is the case in Fig. 4c where the index of refraction is such that there are islands in the surface of section at the minima of the relevant adiabatic curve. Then the chaotic trajectories circulate around the outside of the islands (Fig. 2a). In
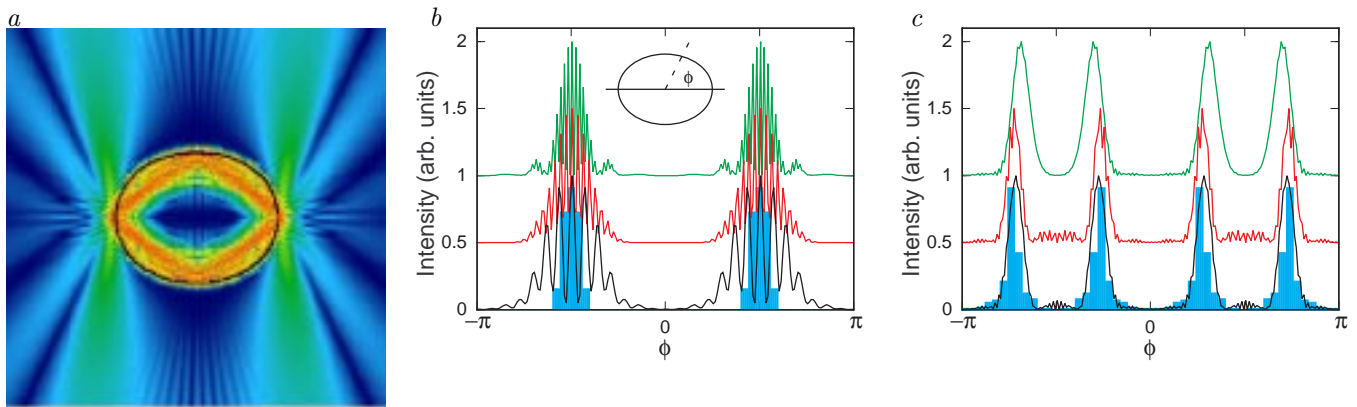
3

FIG. 4 *a* False color representation of the electric field intensity in the TM mode for the $kR = 45.15$ resonance at $\epsilon = 0.11$ determined from the exact numerical solution. Intensity is higher for redder colors, and vanishes in the dark blue regions. One clearly sees the high intensity regions in the near-field just outside the surface at the highest curvature points $\phi = 0, \pi$, and the high emission intensity lines (green) emanating from these points in the tangent directions. *b* Far-field plots of the intensity of three resonances with $kR = 12.1, \sin\chi \approx 0.8$ (black); $kR = 27.9, \sin\chi \approx 0.9$ (red); $kR = 45.4, \sin\chi \approx 0.75$ (green). Index of refraction is $n = 2$ (offset for clarity). Blue histogram is the prediction of the ray-optics model. Note two peaks at $\phi = \pm\pi/2$, corresponding to the tangent directions to the points of highest curvature. *c* Far-field plots for three resonances with $kR = 57.8, \sin\chi \approx 0.8$ (black); $kR = 48.4, \sin\chi \approx 0.91$ (red); $kR = 45.7, \sin\chi \approx 0.91$ (green); compared to the ray-optics model (blue histogram) for $n = 1.54$. Note that each peak is split and the intensity is negligible in the direction tangent to the points of highest curvature. This arises from the presence of stable islands eclipsing the points of highest curvature for $n = 1.54$ as shown in Fig. 2a.

this case the peaks split and maximum emission does not occur at the points of highest curvature. All these ray-optics predictions are seen to be in agreement with the wave solutions.

These compact dielectric resonators with controllable Q and highly directional emission may well be useful for applications to microlasers and fibre-optic communications.

[1] Yamamoto, Y., and Slusher, R. E., Physics Today **46**, 66-73 (1993).
[2] Nöckel, J. U., Stone, A. D. & Chang, R. K., Optics Letters **19**, 1693-1695 (1994).
[3] Mekis, A., Nöckel, J. U., Chen, G., Stone, A. D. & Chang, R. K., Phys. Rev. Lett. **75**, 2682-2685 (1995).
[4] Nöckel, J. U. & Stone, A. D., in: *Optical Processes in Microcavities* (ed. Chang, R. K. & Campillo, A. J.) 389-426, (World Scientific Publishers, Singapore, 1996).
[5] Johnson, B. R., J. Opt. Soc. Am. **10**, 343-352 (1993).
[6] Bohigas, O., Boosé, D., Egydio de Carvalho, R. & Marvulle, V. , Nucl. Phys. A **560**, 197-214 (1993).
[7] Doron, E. & Frischat, S. D., Phys. Rev. Lett. **75** 3661-3664 (1995).
[8] Casati, G., Chirikov, B. V., Guarneri, I. & Shepelyansky, D. L., Phys. Rev. Lett. **56**, 2437-2440 (1986).
[9] Berry, M. V., Eur. J. Phys. **2**, 91-102 (1981).
[10] Lazutkin, V. F., *KAM Theory and Semiclassical Approximations to Eigenfunctions* (Springer, Berlin, 1993).
[11] Robnik, M., J. Phys. A **16**, 3971-3986 (1983).
[12] Gutzwiller, M. C., *Chaos in Classical and Quantum Mechanics* (Springer, Berlin, 1990).
[13] Robnik, M. & Berry, M. V., J. Phys. A: Math. Gen. **18**, 1361-1378 (1985).
[14] Keller, J. B. & Rubinow, S. I., Ann. Phys. **9**, 24-75 (1960).
[15] Nöckel, J. U., Stone, A. D., Chen, G., Grossman, H. & Chang, R. K., Opt. Lett. **21**, 1609-11 (1996).